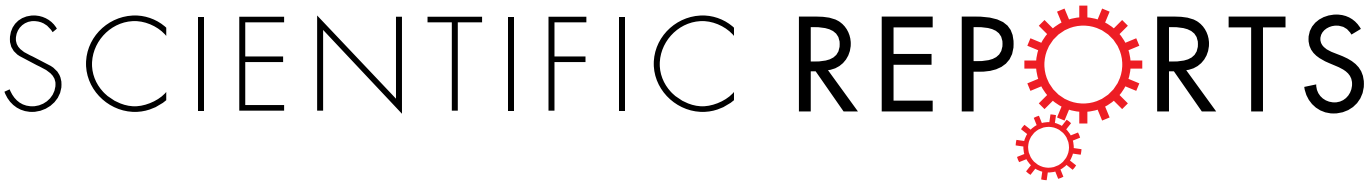

OPEN

Large Scale Synthesis of NiCo Layered Double Hydroxides for Superior Asymmetric Electrochemical Capacitor

Received: 17 September 2015
Accepted: 25 November 2015
Published: 12 January 2016

Ruchun Li, Zhaoxia Hu, Xiaofeng Shao, Pengpeng Cheng, Shoushou Li, Wendan Yu, Worong Lin & Dingsheng Yuan

We report a new environmentally-friendly synthetic strategy for large-scale preparation of 16 nm-ultrathin NiCo based layered double hydroxides (LDH). The $Ni_{50}Co_{50}$-LDH electrode exhibited excellent specific capacitance of 1537 F g^{-1} at 0.5 A g^{-1} and 1181 F g^{-1} even at current density as high as 10 A g^{-1}, which 50% cobalt doped enhances the electrical conductivity and porous and ultrathin structure is helpful with electrolyte diffusion to improve the material utilization. An asymmetric ultracapacitor was assembled with the N-doped graphitic ordered mesoporous carbon as negative electrode and the NiCo LDH as positive electrode. The device achieves a high energy density of 33.7 Wh kg^{-1} (at power density of 551 W kg^{-1}) with a 1.5 V operating voltage.

Ultracapacitors (UCs) are attractive energy storage devices, due to their high power density and excellent cycling stability[1–4]. They have been widely used in electrical vehicles and microelectronic devices. Carbon based materials such as graphene[5–7], carbon nanotubes[8] and activated carbon[9] are the most commonly used electrodes for electrochemical double layer (EDL) ultracapacitors. However, relatively low specific capacitance (~200 F g^{-1}) is the major drawback for EDL capacitors. Alternatively, metal oxide[10–15], metal hydroxide[16,17], layered double hydroxides[5,18,19] and conducting polymers[12,20–23] are commonly used as pseudocapacitive materials. They store charges via superficial Faradic reactions and exhibit higher specific capacitance than EDL materials.

Among these pseudocapacitive materials, NiO and $Ni(OH)_2$ have attracted a lot of attention due to their high theoretical capacitance, excellent chemical stability, low cost and low toxicity. For example, β-$Ni(OH)_2$ achieved its theoretical value of specific capacitance up to 2358 F g^{-1} at a voltage of 0.44 V[17]. However, the relatively poor electrical conductivity (0.01~0.32 S m^{-1})[24] of $Ni(OH)_2$ or NiO is the major drawback as the electrode material. Thus, cobalt was introduced in $Ni(OH)_2$ or NiO to improve the conductivity of electrode materials[25] and raise the oxygen overpotential helpful with widening potential window[18]. It has been reported that Co^{2+} can be oxidized to conductive CoOOH during discharge process, resulting in the increase of conductivity of electrode materials[26]. Besides, the slow kinetics of Faradic reactions of NiCo based materials is another factor that limits their electrochemical performance[27]. It is desirable to develop NiCo based electrodes with large ion accessible surface area. Previous studies have primarily been focused on development of NiCo based nanomaterials with controlled morphology and enhanced surface area, such as nanorods[3], nanowires[28], and nanosheets[29]. However, the large scale synthesis of these nanostructures is rarely reported, while it is critical for practical applications.

Here we developed a large-scale and environmentally-friendly strategy to prepare ultrathin 2-dimensional (2D) porous $Ni(OH)_2$-$Co(OH)_2$ layered double hydroxide. To the best of our knowledge, this is the first report on the large-scale production of NiCo based LDH in a homogeneous ethylene glycol-water system. In comparison to the traditional oil/water methods, which use toxic or flammable solvents such as 1-butanol, toluene, formamide, dimethyl formamide (DMF) and dimethyl sulfoxide (DMSO)[30], our approach involving non-toxic ethylene glycol-water as the solvent system is more environmentally friendly. Moreover, the as prepared porous, ultrathin LDH nature provides extremely large ion-accessible surface area, which improves the kinetics of superficial Faradic reaction. Asymmetric ultracapacitors using $Ni_{50}Co_{50}$-LDH electrode with a high mass loading of 8 mg as cathode and N-doped graphitic ordered mesoporous carbon (GOMC) as anode showed excellent performance in charge storage.

Department of Chemistry, Jinan University, Guangzhou 510632, PR China. Correspondence and requests for materials should be addressed to D.S.Y. (email: tydsh@jnu.edu.cn)

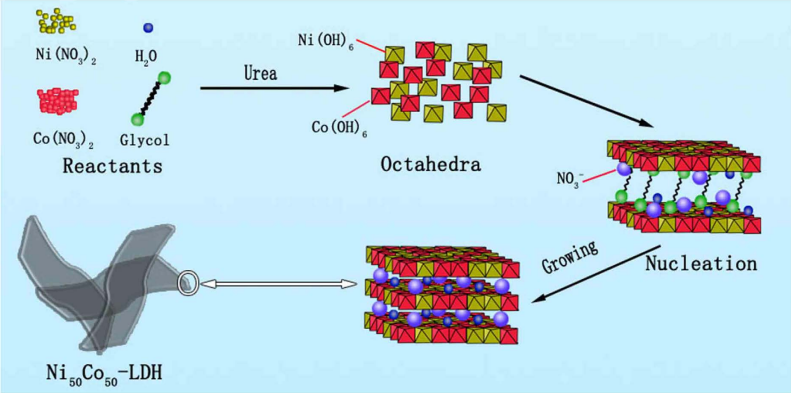

Figure 1. Schematic illustration of growth mechanism of $Ni_{50}Co_{50}$-LDH.

Results

A new synthetic method was used to prepare NiCo-LDHs and $Ni(OH)_2$ and $Co(OH)_2$ in a homogeneous ethylene glycol-water system. The ultrathin 2D nanostructure was obtained for these materials. Among them, $Ni_{50}Co_{50}$-LDH exhibited excellent electrochemical performance, being listed in Table S1 (Support Information, SI). Therefore, $Ni_{50}Co_{50}$-LDH was mainly characterized the structure and perform the electrochemical measurement. The synthetic mechanism was illustrated in Fig. 1. Ammonia was gradually generated by the hydrolysis of urea (Eq. 1). Then NH_3 molecules reacted with Ni and Co metal ions and formed complexes (Eq. 2). Excess amount of NH_3 molecules produced OH^- and the nickel and cobalt ions were formed $Ni(OH)_6$ and $Co(OH)_6$ octahedra with OH^- (Eq. 3 and 4).

$$CO(NH_2)_2 + 2H_2O \leftrightarrow H_2CO_3 + NH_3 \quad (1)$$

$$Ni^{2+} + 6NH_3 \leftrightarrow [Ni(NH_3)_6]^{2-};\ Co^{2+} + 6NH_3 \leftrightarrow [Co(NH_3)_6]^{2+} \quad (2)$$

$$NH_3 + H_2O \leftrightarrow NH^{4+} + OH^- \quad (3)$$

$$OH^- + Ni^{2+} \leftrightarrow Ni(OH)_2;\ 2OH^- + Co^{2+} \leftrightarrow Co(OH)_2 \quad (4)$$

$Ni(OH)_6$ and $Co(OH)_6$ octahedra nuclei were self-assembled to form the infinite 2D sheets composed of metal cations occupy the centre of octahedra's edge and hydroxide ions at vertexes. These 2D sheets further extended and form the $Ni_{50}Co_{50}$-LDH nanosheets. The nanosheets were washed with ethanol and water. It is expected that H_2O molecules and NO_3^- ions will be retained within the interlayer space of LDH through hydrogen bond. Importantly, 10 gram scale of $Ni_{50}Co_{50}$-LDH can be readily prepared by this simple synthetic method (Fig. S1, SI), which holds great promise for mass production.

The morphology of as-prepared samples was characterized by SEM and TEM techniques. SEM images in Fig. S2 showed that ultrathin nanosheets were about a thickness of ~16 nm. TEM, HRTEM images and the selected-area electron diffraction (SAED) patterns of α-$Ni(OH)_2$,α-$Co(OH)_2$ and $Ni_{50}Co_{50}$-LDH were shown in Fig. 2. TEM images confirmed that this method could be used to prepare the ultrathin nanosheets transition metal hydroxides and LDHs (Fig. 2a,c,e). In the HRTEM images, lattice fringes were observed on the nanosheets (Fig. 2b,d,f). At the same time, the SAED patterns collected from the nanosheet also exhibited diffraction rings but vague spots, indicating the crystallinity of these samples is relatively low. In addition, some pore structure was also found, which will be advantageous to the electrolyte diffusion.

The crystal structure of $Ni_{50}Co_{50}$-LDH and α-$Ni(OH)_2$ and α-$Co(OH)_2$ were further characterized by XRD analysis. As shown in Fig. 3a, the $Ni_{50}Co_{50}$-LDH sample exhibited diffraction peaks centered at 11.6°, 23.9°, 34.4° and 60.5° that can be indexed as the (003), (006), (012) and (110) planes of nickel cobalt carbonate hydroxide hydrate (JCPDS 33–0429). The diffraction peaks obtained for $Ni(OH)_2$ sample are 12.1°, 24.0°, 33.5°, 35.4° and 59.8°, which can be ascribed to the (001), (002), (110), (111), and (300) planes of layered nickel hydroxide hydrate [α-3 $Ni(OH)_2 \bullet H_2O$, JCPDS 22–0444]. As-prepared cobalt hydroxide was low-crystalline α-hydroxides in good agreement with previous reported results[31,32] showing typical low-crystalline α-hydroxides with weak diffraction peaks of (003), (006) and (012) planes in the XRD patterns. The low crystallinity is in accordance with the above-mentioned HRTEM and SAED characterization.

Figure 3b shows the FTIR spectra of $Ni_{50}Co_{50}$-LDH, α-$Ni(OH)_2$ and α-$Co(OH)_2$ samples. They have similar IR bands. The signal at 3453 cm^{-1} is the O-H stretching band, arising from interlayer water molecules and metal-hydroxyl groups. The band centered at 1634 cm^{-1} can be ascribed to the bending vibration of water. Additionally, the band at 1388 cm^{-1} can be assigned to the vibration of interlayer CO_3^{2-} and NO_3^- anions. CO_3^{2-} participated to form the nickel cobalt carbonate hydroxide hydrate with Ni^{2+} and Co^{2+} ions via coordinate bonds

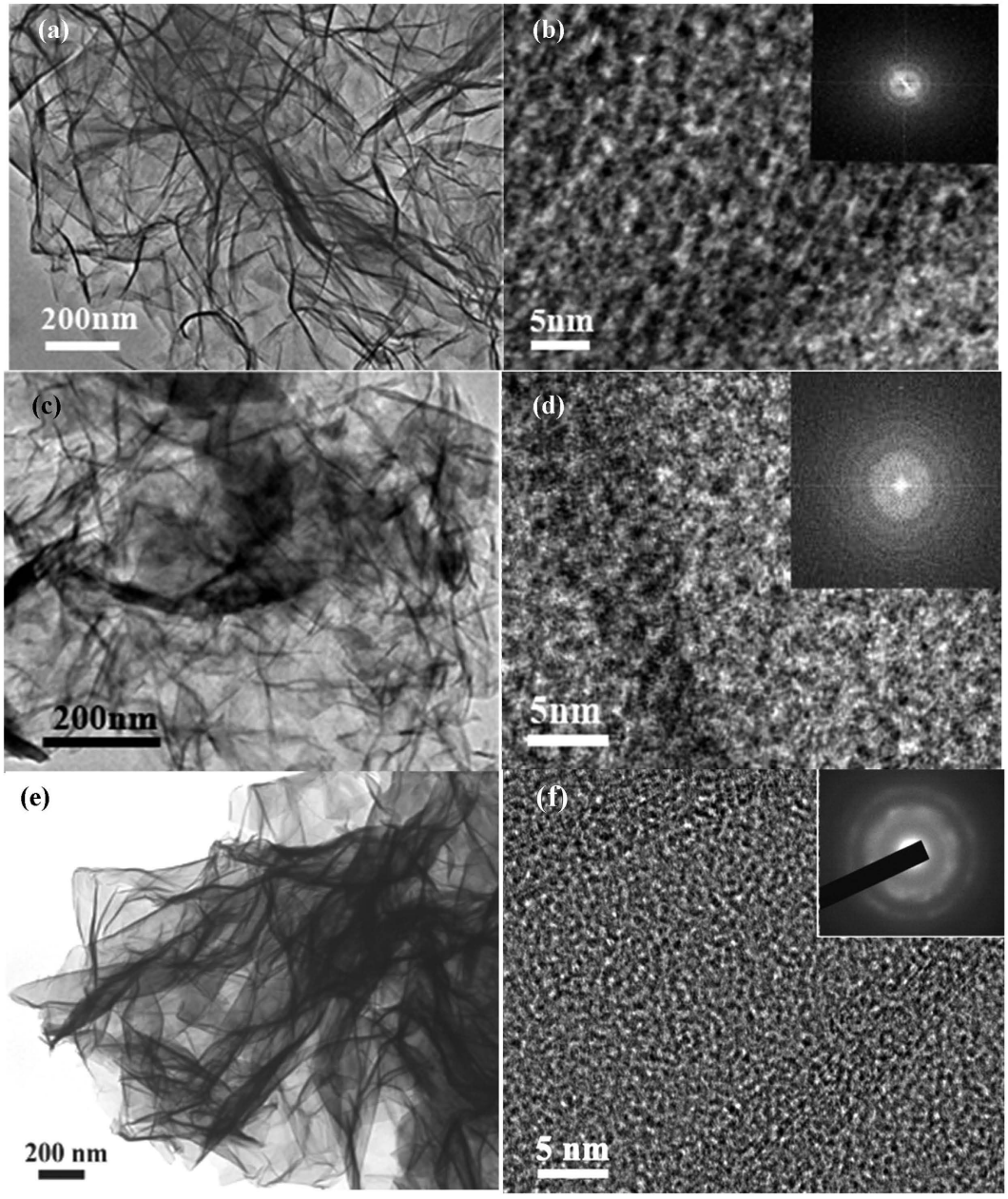

Figure 2. TEM, HRTEM images and SAED patterns of as-prepared samples. α-$Ni(OH)_2$ (**a**,**b**), α-$Co(OH)_2$ (**c**,**d**), $Ni_{50}Co_{50}$-LDH(**e**,**f**).

while NO_3^- retained in the interlayer of LDH. The broad peak at 634 cm^{-1} can be assigned to the M–O, O–M–O, and M–O–M (M=Co and Ni) vibrations[32,33].

Figure S3a and b show the N_2 adsorption–desorption isotherms and the corresponding Barret-Joyner-Halenda (BJH) pore size distribution of these samples, respectively. The samples presented a type III curve with H1 hysteresis loop at high relative pressure, indicating the presence of macropores and mesopores. The adsorption isotherms became rapidly saturated at low relative pressure, illustrating the low adsorption volume of metal oxides or LDHs. A platform at $P / P_0 = 0.20–0.80$ originated from the outer superfacial adsorption of nanosheets, contributing the low adsorption volume. In addition, a hysteresis loop at a higher relative pressure ($P / P_0 = 0.80–0.99$) was obtained. This loop resulted from the macroporous adsorption among the overlap gaps of the nanosheets. It was noted that the desorption branch of LDH showed type IV with H2 hysteresis loop, suggesting the existence of mesoporous structure. The BET surface areas of the $Ni_{50}Co_{50}$-LDH, α-$Co(OH)_2$ and α-$Ni(OH)_2$ were 80, 97 and 119 m^2g^{-1}, respectively, and the average pore size was mainly less than 10 nm. On the other hand, the ion radii (74pm) of Co^{2+} is larger than 72 pm of Ni^{2+}, thus with cobalt doping, the interlayer distance was widened and facilitate ion transfer. Nitrogen absorption-desorption measurement indicates that the specific surface of LDHs is increased with the increase of cobalt contents and confirms the presence of mesoporous loop (see Fig. S4).

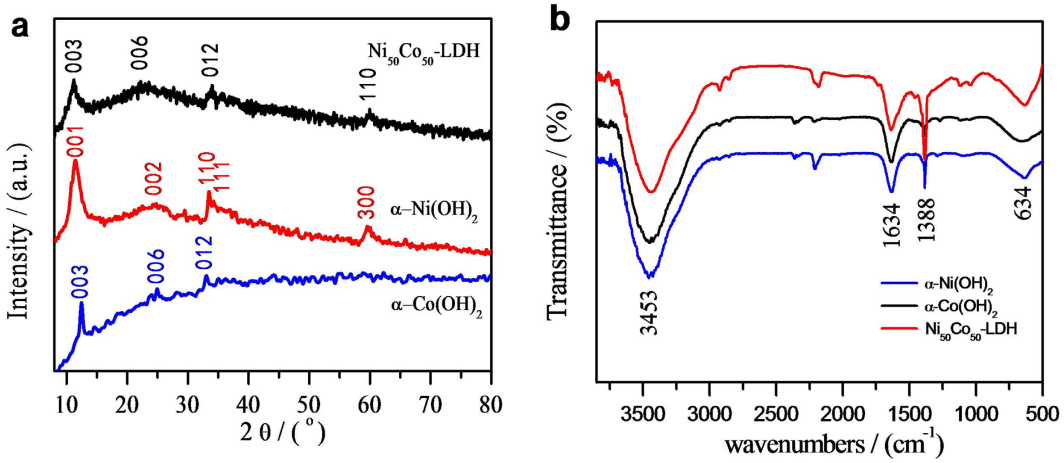

Figure 3. (**a**) XRD patterns and (**b**) FT-IR spectra of the $Ni_{50}Co_{50}$-LDH and α-$Ni(OH)_2$ and α-$Co(OH)_2$.

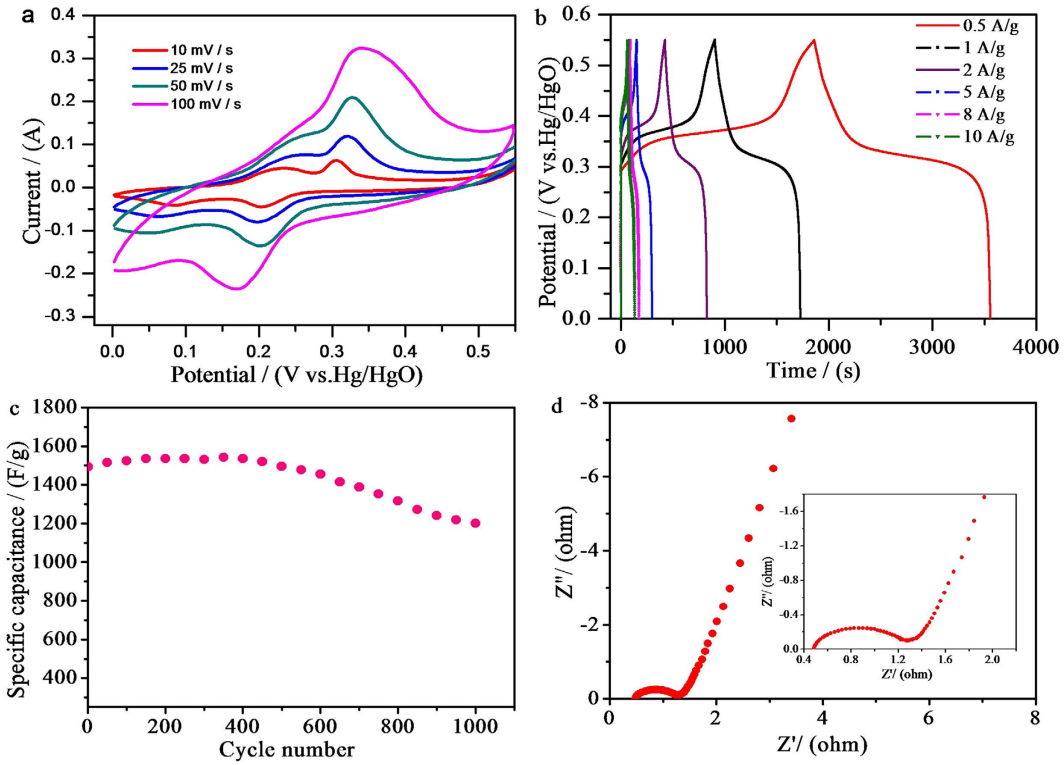

Figure 4. (**a**) CV curves, (**b**) galvanostatic charge/discharge curves, (**c**) cycling stability and (**d**) Nyquist plot of EIS analysis of $Ni_{50}Co_{50}$-LDH in 6 mol L^{-1} KOH electrolyte.

Electrochemical measurements were carried out to study the charge storage performance of the $Ni_{50}Co_{50}$-LDH samples in 6 mol L^{-1} KOH electrolyte. Figure 4a shows the CV curves for the LDH electrode at different scan rates. A set of distinct redox peaks were observed between 0.1 V and 0.5 V vs. Hg/HgO, which are consistent with the capacitive behavior reported for $Ni(OH)_2$ and $Co(OH)_2$[34,35]. The current intensity increased almost linearly with the increase of scan rate, implying excellent reversibility and rapid charge-discharge response[36,37].

The mechanisms of electric energy storage for pseudo-capacitor are proposed as follows (Eq. 5–7). The pseudo-capacitance of LDH is attributed from both α-$Co(OH)_2$ and α-$Ni(OH)_2$. Redox reactions of α-$Co(OH)_2$ contain two steps as shown in Fig. 5a. The electrons were transported among Co^{2+}, Co^{3+} and, Co^{4+} ions with the protons transfer (Eq. 5 and 6). Equation 7 illustrates the charge/discharge mechanism of $Ni(OH)_2$.

$$Co(OH)_2 + OH^- \leftrightarrow CoOOH + H_2O + e^- \quad (5)$$

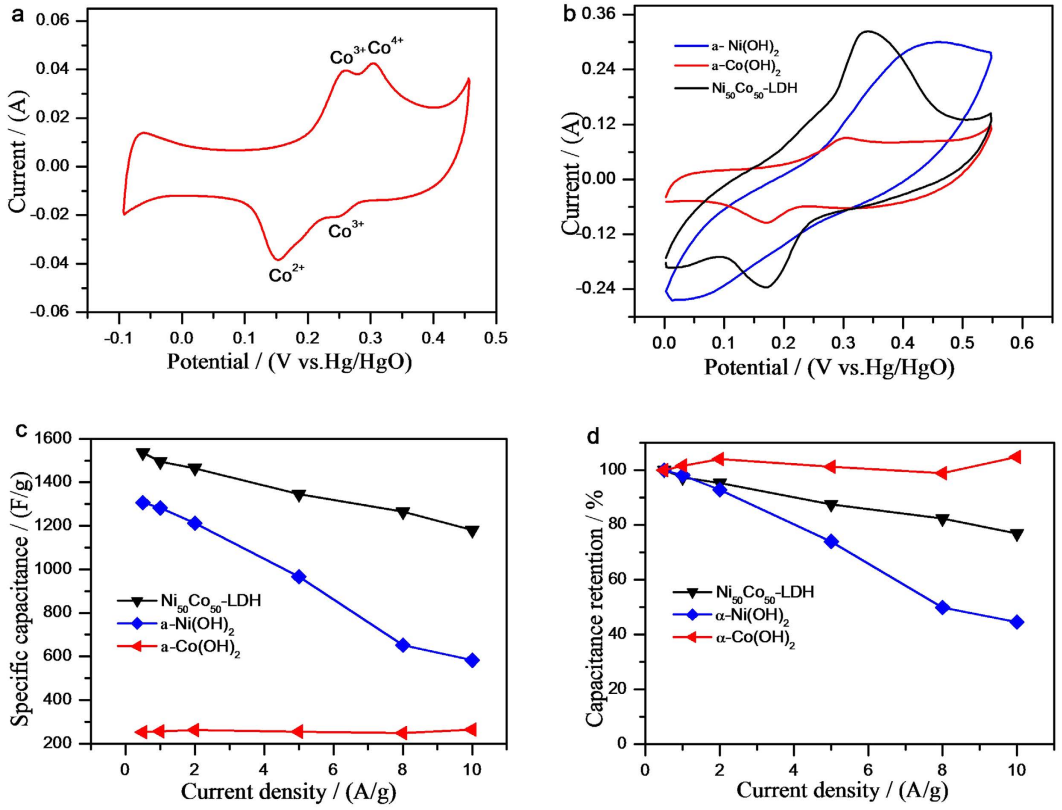

Figure 5. CV curve of (**a**) α-$Co(OH)_2$ at 10 mV s^{-1} and (**b**) the $Ni_{50}Co_{50}$-LDH, α-$Ni(OH)_2$ and α-$Co(OH)_2$ at 100 mV s^{-1} . The (**c**) compared specific capacitance and (**d**) the capacitance retention for $Ni_{50}Co_{50}$-LDH, α-$Co(OH)_2$ and α-$Ni(OH)_2$.

$$CoOOH + OH^- \leftrightarrow CoO_2 + H_2O + e^- \quad (6)$$

$$Ni(OH)_2 + OH^- \leftrightarrow NiOOH + H_2O + e^- \quad (7)$$

Figure 4b shows the galvanostatic charge-discharge curves of the LDH electrode at different current densities. As a typical battery material, the LDH showed almost symmetrical charge and discharge curves, indicating fast and good electrochemical reversibility. The specific capacitance of the LDH achieved excellent initial specific capactance of 1537 F g^{-1} at 0.5 A g^{-1} and 1181 F g^{-1} even at current density as high as 10 A g^{-1}. A 1000-cycle stability curve collected at 2 A g^{-1} is shown in Fig. 4c. The initial specific capacitance was 1494 F g^{-1}, the value slowly increased to a maximal value of 1542 around 400th cycle, which was attributed to the activation of Ni-based electrode materials[38]. The retention of the specific capacitance was 80.3% after 1000 cycles. Electrochemical impedance spectroscopy (EIS) was carried out to evaluate the diffusion of electrolyte ions to porous structure and charge transfer at the interface of LDH (Fig. 4d). The impedance plots exhibited two distinct parts including a semicircle in the high-frequency region and a sloped line in the low-frequency region. The charge transfer resistance (R_{ct}) was estimated to be ~0.8 Ω from the semicircle diameter at the high-frequency. The small R_{ct} could be attributed to the ultrathin nanosheets morphology, which allows efficient charge transfer between the electrolyte and LDH. In addition, the solution resistance (R_s) was estimated to be ~0.48 Ω from the left intersection point of the semi-circle and Z'-axis. The low R_{ct} and R_s as well as high specific capacitance support that the $Ni_{50}Co_{50}$-LDH is an excellent capacitive electrode material for ultracapacitors.

The specific capacitance and capacitance retention were measured for $Ni_{50}Co_{50}$-LDH, α-$Co(OH)_2$ and α-$Ni(OH)_2$ using galvanostatic charge/discharge. As shown in Fig. 5c,d, the specific capacitance of LDH is substantially larger than that of α-$Ni(OH)_2$ and α-$Co(OH)_2$ (Fig. 5c). The capacitance of α-$Ni(OH)_2$ rapidly decreased with the increase of current density. However, the capacitance retention of α-$Co(OH)_2$ at 10 A g^{-1} is lightly over that at 0.5 A g^{-1} (see Fig. 5d). Though the specific capacitance of α-$Co(OH)_2$ is much less than that of pure α-$Ni(OH)_2$, 50% cobalt-doped α-$Ni(OH)_2$ ($Ni_{50}Co_{50}$-LDH) visibly exhibits excellent electrochemical performance, involving superior specific capacitance and the capacitance retention to pure α-$Ni(OH)_2$. This is also confirmed by the other reseaches. Lang *et al.* obtained $Ni_{44}Co_{56}$ oxide nanoflakes with a maximum specific capacitance of 1227 F g^{-1} at 0.625 A g^{-1} based on 0.4 V operating potential[39]. When the atom ratio of nickel and cobalt is close to 1:1, these kinds of materials exhibit the superior electrical conductivity[25]. Cobalt was introduced in LDH to improve the conductivity of electrode materials[25] and raise the oxygen overpotential advantageous to widening potential window[18]. Co^{2+} were oxidized to form the conductive CoOOH in discharge process, resulting in the increase of

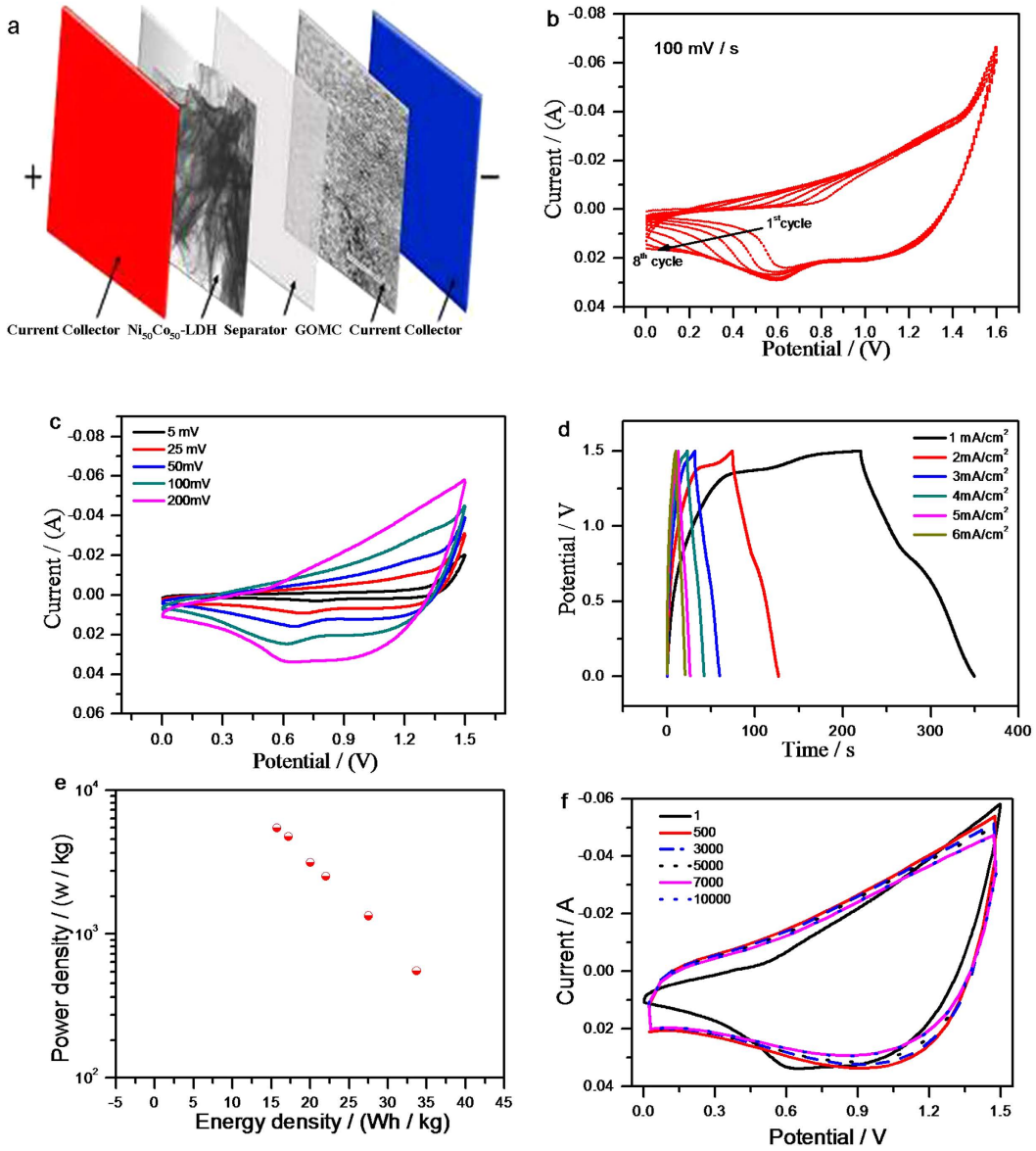

Figure 6. (**a**) Schematic illustration of GOMC//$Ni_{50}Co_{50}$-LDH device. (**b**) 1st~8th CV curves, (**c**) CV curves at different scan rates. (**d**) Galvanostatic charge/discharge curves. (**e**) Ragone plots of GOMC//$Ni_{50}Co_{50}$-LDH. (**f**) CV curves from cycling-stability measurement for GOMC//$Ni_{50}Co_{50}$-LDH in 6 mol L^{-1} KOH aqueous electrolyte.

conductivity of electrode materials[26]. Due to the cobalt introduced to participate in the electrochemical redox reaction, good conductivity improves the charge transfer and low R_{ct} and R_s are helpful with Faradic reaction, resulting in $Ni_{50}Co_{50}$-LDH presents high performance in electrochemical energy storage than nickel hydroxide. The comparable CV curves for the LDH and α-$Ni(OH)_2$ and α-$Co(OH)_2$ at 100 mV s^{-1} is shown in Fig. 5b. The serious polarization is shown in CV curve of α-$Ni(OH)_2$. The reversibility of LDH is visibly improved due to cobalt doped, which is helpful with the Columbic efficiency and the materials utilization.

The potential window of $Ni_{50}Co_{50}$-LDH is relatively small (~0.55 V), which seriously limit its practical application. In order to enlarge the operating voltage window, we fabricated an asymmetric device using GOMC as negative electrode and $Ni_{50}Co_{50}$-LDH as positive electrode (denoted as GOMC//$Ni_{50}Co_{50}$-LDH), as shown in Fig. 6a. GOMC is a promising negative electrode material that has long cycling stability and 1.0 V operating potential window in alkaline electrolyte[40]. The CV of GOMC presented a typical rectangular shape in agreement with its electric double-layer capacitive behavior.

The designated asymmetric capacitor has an optimal operating voltage of 1.5 V. When the voltage reached 1.6 V, water splitting occurs and the current drastically increased (Fig. 6b and Fig. S5b). For asymmetric UCs, the charges on anode and cathode should be balanced ($q+ = q-$). This can be achieved by manipulating the mass loading of active materials on each electrode. According the following equation, the total charge (q) of one electrode stored is depending on the specific capacitance (C), the potential window (ΔE) and the mass of the electrode (m)[41,42].

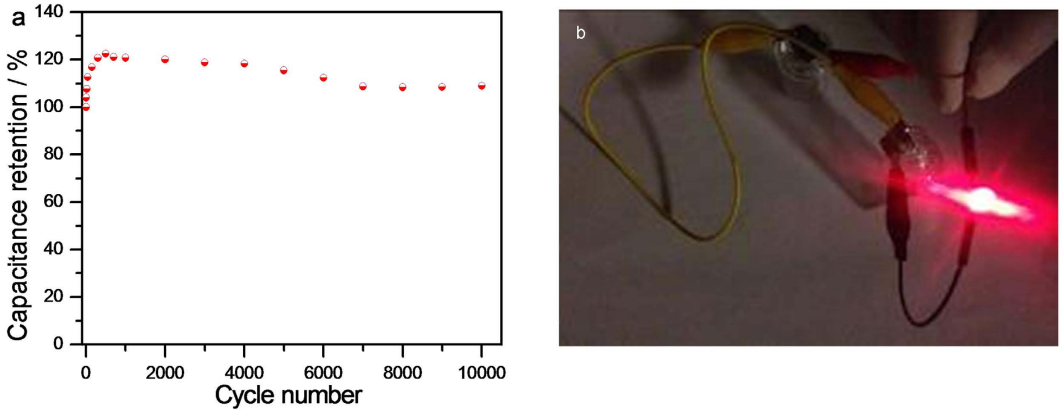

Figure 7. (**a**) Cycling stability for GOMC//$Ni_{50}Co_{50}$-LDH device; (**b**) A red LED (1.5 V) was powered by the device.

$$q = C \times \Delta E \times m \tag{8}$$

Therefore, the ratio of mass loading of negative and positive electrode materials can be calculated by Eq. 9.

$$m_+/m_- = C_- \times \Delta E_-/(C_+ \times \Delta E_-) \tag{9}$$

Based on the data of the specific capacitances and potential windows of two electrodes, the optimal mass ratio between GOMC and LDH was 5:1.

Cyclic voltammetry and galvanostatic charge/discharge measurements were collected from the asymmetric UC device. As shown in Fig. 6b, the capacitance of GOMC//$Ni_{50}Co_{50}$-LDH asymmetric UC increase gradually due to the activation of nickel hydroxide. Figure 6c shows CV curves measured at different scan rates, the large area of different curves clarified superior performance of this device. Galvanostatic charge/discharge curves were conducted at different current densities (Fig. 6d) to evaluate the capacitance, power density and energy density of asymmetric device. Areal capacitances of 86.3, 70.4, 56.4, 51.2, 44.0 and 40.3 F cm^{-2} were obtained at 1, 2, 3, 4, 5 and 6 mA cm^{-2}, which correspond to gravimetric capacitance of 107.8, 88.0, 70.5, 64, 55 and 50.4 F g^{-1}, respectively. The Ragone plot for the device is presented in Fig. 6e. The device achieved an excellent energy density of 33.7 Wh kg^{-1} and a high power density of 5.4 kW kg^{-1} (see Formula, SI).

Cycling stability is a key factor for evaluating the device performance in practical application. Figure 6f shows the CV curves collected at 200 mV s^{-1} as a function of number of cycles. The capacitance quickly increased in the first 500 cycles, which is in good agreement with the $Ni_{50}Co_{50}$-LDH electrode performance measured in 3-electrode system. Thereafter, the capacitance decrease gradually. The specific capacitance retention rate was 109% after 10000 cycles (Fig. 7a). The asymmetric device exhibits high specific energy density and excellent cycling stability. These excellent electrochemical performances could be attributed to: (i) the ultrathin and porous nature of $Ni_{50}Co_{50}$-LDH and (ii) fast charge transfer, rapid mass transport and anti-corrosion of GOMC. Moreover, GOMC//$Ni_{50}Co_{50}$-LDH device could successfully power a red light-emitting-diode (LED) with a nominated voltage of 1.5 V for over 6 min after charging with current density of 4 mA cm^{-2} (Fig. 7b).

Discussions

Based on the above analysis, it could be found the ultrathin $Ni_{50}Co_{50}$-LDH has been successfully synthesized by the efficient and low cost strategy. The morphology characterizations showed that ultrathin nanosheets were about a thickness of ~16 nm and the electrochemical results reveal that $Ni_{50}Co_{50}$-LDH possesses high specific capacitance. The ultrathin porous nanostructure can not only be beneficial for efficient ion and electron transport but also improve specific surface area to increase active sites for the energy storage. In addition, the excellent conductivity of as-prepared material has demonstrated by the EIS testing which may also attribute to the enhanced capacitance.

In summary, we have demonstrated a scalable and environmentally-friendly strategy for large-scale preparation of ultrathin $Ni_{50}Co_{50}$-LDH. The $Ni_{50}Co_{50}$-LDH exhibited high pseudo-capacitance and kinetic properties to be used as the cathode materials for electrochemical energy storage. Therefore, we have developed the asymmetric capacitor composed of $Ni_{50}Co_{50}$-LDH and GOMC, which exhibits wide operating voltage of 1.5 V, excellent stability (109% capacitance retention after 10000 cycles), high energy density (33.7 Wh kg^{-1}) and power density (5452 W kg^{-1}). We believe this novel strategy can be extended to prepare other ultrathin 2D capacitive materials for charge storage devices.

Methods

Preparation of NiCo layered double hydroxides. The NiCo LDH was prepared by the following optimal procedure. 2.5 mmol of $Ni(NO_3)_2 \cdot 6H_2O$ and 5 mmol of $Co(NO_3)_2 \cdot 6H_2O$ (Ni:Co = 1:2) were dissolved in a mixture solvent of 37.5 mL ethylene glycol and 15 mL deionized water. Then, 37.5 mmol of urea was added under stirring. The resulting solution was transferred into in a round-bottom flask to be refluxed under vigorous magnetic stirring for 3 h at 90 °C. Then, the precipitates were filtered and washed several times with distilled water and ethanol, and

then dried at 60 °C. The as-prepared sample was denoted as $Ni_{50}Co_{50}$-LDH. The same experimental procedures were also employed to prepare ultrathin $Ni(OH)_2$, $Ni_{79}Co_{21}$-LDH, $Ni_{76}Co_{24}$-LDH, $Ni_{64}Co_{46}$-LDH, $Ni_{35}Co_{65}$-LDH and $Co(OH)_2$ by changing the ratio of the nickel and cobalt source.

Characterization. Powder X-ray diffraction measurements were performed by a MSAL-XD2 X-ray diffractometer (Cu $K\alpha$, 36 kV, 20 mA, $\lambda = 1.5406$ Å). The morphologies of LDH samples were examined by field-emission scanning electron microscope (SEM) (FSEM, ZEISS Ultra 55) and high resolution transmission electron microscope (TEM) (HRTEM, JEOL JEM-2100F) with an accelerating voltage of 200 kV. The FT-IR spectra were collected by a Nicolet 6700 FT-IR spectrometer. Nitrogen sorption isotherms of samples were collected by a Micromeritics TriStar 3000 Analyzer at 77 K. Elemental analysis was performed by the inductively coupled plasma optical emission spectrometer (Perkin Elmer, optima 2000DV), indicating the Ni/Co atom ratio of LDH.

Electrochemical measurements. Working electrode was fabricated by sandwiching the mixture of active materials (8 mg), carbon black and PTFE (with a mass ratio of 80:15:5) between two pieces of nickel foams. The mass loading of the electrode was measured by the mass difference before and after sandwiching. A nickel foil and an Hg/HgO electrode were used as current collector and reference electrode, respectively. All electrochemical measurements were performed on a CHI660D electrochemical workstation in a standard three electrodes cell at room temperature. Cyclic voltammetry (CV), galvanostatic charge-discharge and electrochemical impedance spectroscopy (EIS) tests were all performed in 6 mol L^{-1} KOH aqueous solution. EIS analysis was performed at the frequency range of 100 kHz ~0.1 Hz with amplitude of 5 mV. Asymmetric capacitors were fabricated by using N-doped graphitic ordered mesoporous carbon (GOMC) as negative electrode and $Ni_{50}Co_{50}$-LDH as positive electrode, and their electrochemical performance was measured in 6 mol L^{-1} KOH aqueous solution by a 2-electrode cell system.

References

1. Wang, W. *et al.* A Novel Exfoliation Strategy to Significantly Boost the Energy Storage Capability of Commercial Carbon Cloth. *Adv. mater.* **27,** 3572–3578 (2015).
2. Ci, S. *et al.* NiO-Microflower Formed by Nanowire-weaving Nanosheets with Interconnected Ni-network Decoration as Supercapacitor Electrode. *Sci. Rep*. **5,** 11919 (2015).
3. Choi, H. J. *et al.* Graphene for energy conversion and storage in fuel cells and supercapacitors. *Nano Energy* **1,** 534–551 (2012).
4. Abushrenta, N., Wu, X., Wang, J., Liu, J. & Sun, X. Hierarchical Co-based Porous Layered Double Hydroxide Arrays Derived via Alkali Etching for High-performance Supercapacitors. *Sci. Rep*. **5,** 13082 (2015).
5. Zou, Y. & Wang, S. Interconnecting Carbon Fibers with the *In-situ* Electrochemically Exfoliated Graphene as Advanced Binder-free Electrode Materials for Flexible Supercapacitor. *Sci. Rep*. **5,** 11792 (2015).
6. Lin, T. W., Dai, C. S. & Hung, K. C. High energy density asymmetric supercapacitor based on NiOOH/Ni_3S_2/3D graphene and Fe_3O_4/graphene composite electrodes. *Sci. Rep*. **4,** 7274 (2014).
7. Yu, G. *et al.* Enhancing the supercapacitor performance of graphene/MnO_2 nanostructured electrodes by conductive wrapping. *Nano Let*. **11,** 4438–4442 (2011).
8. Wang, G. *et al.* Enhanced capacitance in partially exfoliated multi-walled carbon nanotubes. *J. Power Sources* **196,** 5209–5214 (2011).
9. Gamby, J., Taberna, P. L., Simon, P., Fauvarque, J. F. & Chesneau, M. Studies and characterisations of various activated carbons used for carbon/carbon supercapacitors. *J. of Power Sources* **101,** 109–116 (2001).
10. Luan, F. *et al.* High energy density asymmetric supercapacitors with a nickel oxide nanoflake cathode and a 3D reduced graphene oxide anode. *Nanoscale* **5,** 7984–7990 (2013).
11. Lu, X. *et al.* Hydrogenated TiO_2 nanotube arrays for supercapacitors. *Nano Lett.* **12,** 1690–1696 (2012).
12. Chen, L. *et al.* Synthesis and pseudocapacitive studies of composite films of polyaniline and manganese oxide nanoparticles. *J. Power Sources* **195,** 3742–3747 (2010).
13. Wang, G. M. *et al.* LiCl/PVA Gel Electrolyte Stabilizes Vanadium Oxide Nanowire Electrodes for Pseudocapacitors. *Acs Nano* **6,** 10296–10302 (2012).
14. Yu, G. *et al.* Solution-processed graphene/MnO_2 nanostructured textiles for high-performance electrochemical capacitors. *Nano Lett.* **11,** 2905–2911 (2011).
15. Xiao, X. *et al.* Fiber-Based All-Solid-State Flexible Supercapacitors for Self-Powered Systems. *ACS Nano* **6,** 9200–9206 (2012).
16. Cheng, J. *et al.* Hierarchical Core/Shell $NiCo_2O_4$@$NiCo_2O_4$ Nanocactus Arrays with Dual-functionalities for High Performance Supercapacitors and Li-ion Batteries. *Sci. Rep*. **5,** 12099, (2011).
17. Lu, Z., Chang, Z., Zhu, W. & Sun, X. Beta-phased $Ni(OH)_2$ nanowall film with reversible capacitance higher than theoretical Faradic capacitance. *Chem. commun.* **47,** 9651–9653 (2011).
18. Xie, L. *et al.* Co_xNi_{1-x} double hydroxide nanoparticles with ultrahigh specific capacitances as supercapacitor electrode materials. *Electrochim. Acta* **78,** 205–211, (2012).
19. Lin, W. R. *et al.* Superior Performance Asymmetric Supercapacitors Based on Flake-like Co/Al Hydrotalcite and Graphene. *Electrochim. Acta* **143,** 331–339 (2014).
20. Luo, J., Ma, Q., Gu, H., Zheng, Y. & Liu, X. Three-dimensional graphene-polyaniline hybrid hollow spheres by layer-by-layer assembly for application in supercapacitor. *Electrochim. Acta* **173,** 184–192 (2015).
21. Yu, G., Xie, X., Pan, L., Bao, Z. & Cui, Y. Hybrid nanostructured materials for high-performance electrochemical capacitors. *Nano Energy* **2,** 213–234 (2013).
22. Yuan, L. *et al.* Polypyrrole-coated paper for flexible solid-state energy storage. *Energy Environ. Sci.* **6,** 470 (2013).
23. Yuan, L. *et al.* Paper-based supercapacitors for self-powered nanosystems. *Angew. Chem. Int. Edit.* **51,** 4934–4938 (2012).
24. Zhi, M., Xiang, C., Li, J., Li, M. & Wu, N. Nanostructured carbon-metal oxide composite electrodes for supercapacitors: a review. *Nanoscale* **5,** 72–88 (2013).
25. Windisch, C. F., Exarhos, G. J., Ferris, K. F., Engelhard, M. H. & Stewart, D. C. Infrared transparent spinel films with p-type conductivity. *Thin Solid Films* **398,** 45–52 (2001).
26. Chen, J., Bradhurst, D. H., Dou, S. X. & Liu, H. K. Nickel hydroxide as an active material for the positive electrode in rechargeable alkaline batteries. *J. Electrochem. Soc.* **146,** 3606–3612 (1999).
27. Chang, Z., Li, H., Tang, H., Yuan, X. Z. & Wang, H. Synthesis of γ-CoOOH and its effects on the positive electrodes of nickel batteries. *Int. J. Hydrogen Energ*. **34,** 2435–2439 (2009).
28. Salunkhe, R. R., Jang, K. & Lee, S. w. & Ahn, H. Aligned nickel-cobalt hydroxide nanorod arrays for electrochemical pseudocapacitor applications. *RSC Adv*. **2,** 3190–3193 (2012).
29. Zhang, G. & David Lou, X. W. Controlled growth of $NiCo_2O_4$ nanorods and ultrathin nanosheets on carbon nanofibers for high-performance supercapacitors. *Sci. rep*. **3,** 1470 (2013).

30. Wang, Q. & O'Hare, D. Recent advances in the synthesis and application of layered double hydroxide (LDH) nanosheets. *Chem. rev.* **112,** 4124–4155 (2012).
31. Wang, W. *et al.* Controllable synthesis and growth mechanism of α-$Co(OH)_2$ nanorods and nanoplates by a facile solution-phase route. *J. Solid State Chem.* **184,** 3299–3302 (2011).
32. Perez-Ramirez, J., Mul, G., Kapteijn, F. & Moulijn, J. A. *In situ* investigation of the thermal decomposition of Co-Al hydrotalcite in different atmospheres. *J. Mater. Chem.* **11,** 821–830 (2001).
33. Ding, Y. S., Xu, L. P., Chen, C. H., Shen, X. F. & Suib, S. L. Syntheses of nanostructures of cobalt hydrotalcite like compounds and Co_3O_4 via a microwave-assisted reflux method. *J. Phys. Chem. C* **112,** 8177–8183 (2008).
34. Cao, L., Xu, F., Liang, Y. Y. & Li, H. L. Preparation of the novel nanocomposite $Co(OH)_2$/ultra-stable Y zeolite and its application as a supercapacitor with high energy density. *Adv. Mater.* **16,** 1853–1857 (2004).
35. Gupta, V., Gupta, S. & Miura, N. Potentiostatically deposited nanostructured Co_xNi_{1-x} layered double hydroxides as electrode materials for redox-supercapacitors. *J. Power Sources* **175,** 680–685 (2008).
36. Yan, J. *et al.* Fast and reversible surface redox reaction of graphene–MnO_2 composites as supercapacitor electrodes. *Carbon* **48,** 3825–3833 (2010).
37. Xia, N. N. *et al.* Microwave synthesis and electrochemical characterization of mesoporous carbon@Bi_2O_3 composites. *Mate. Res. Bull.* **46,** 687–691 (2011).
38. Yuan, C., Zhang, X., Su, L., Gao, B. & Shen, L. Facile synthesis and self-assembly of hierarchical porous NiO nano/micro spherical superstructures for high performance supercapacitors. *J. Mater. Chem.* **19,** 5772–5777 (2009).
39. Lang, J. W., Kong, L. B., Liu, M., Luo, Y. C. & Kang, L. $Co_{0.56}Ni_{0.44}$ Oxide Nanoflake Materials and Activated Carbon for Asymmetric Supercapacitor. *J. Electrochem. Soc.* **157,** A1341–1346 (2010).
40. Yuan, D. S. *et al.* A novel route for preparing graphitic ordered mesoporous carbon as electrochemical energy storage material. *Rsc Adv.* **3,** 5570–5576 (2013).
41. Khomenko, V., Raymundo-Piñero, E. & Béguin, F. Optimisation of an asymmetric manganese oxide/activated carbon capacitor working at 2V in aqueous medium. *J. Power Sources* **153,** 183–190 (2006).
42. Yu, W. D. *et al.* High performance supercapacitor based on Ni_3S_2/carbon nanofibers and carbon nanofibers electrodes derived from bacterial cellulose. *J. Power Sources* **272,** 137–143 (2014).

Acknowledgements

This work was supported by the Key Program Projects of National Natural Science Foundation of China (21031001) and National Natural Science Foundation of China (21376105 and 21576113) and. the Project for Foshan Innovation Group (2014IT100062).

Author Contributions

R.L. and D.Y. conceived the idea and carried out data analyses. R.L. and Z.H. did the experiments. X.S. and W.L. conducted the electrochemical tests. S.L. and P.C. performed SEM and TEM characterizations. R.L. and W.Y. co-wrote the manuscript.

Additional Information

Supplementary information accompanies this paper at http://www.nature.com/srep

Competing financial interests: The authors declare no competing financial interests.

How to cite this article: Li, R. *et al.* Large Scale Synthesis of NiCo Layered Double Hydroxides for Superior Asymmetric Electrochemical Capacitor. *Sci. Rep.* **6**, 18737; doi: 10.1038/srep18737 (2016).